The structure of braitschite, a calcium rare earth borate

CLARE E. ROWLAND,[1] CHRISTOPHER L. CAHILL,[1] AND JEFFREY E. POST[2],*

[1]Department of Chemistry, The George Washington University, Washington, D.C. 20052, U.S.A.
[2]Department of Mineral Sciences, Smithsonian Institution, Washington, D.C. 20560-0119, U.S.A.

ABSTRACT

The crystal structure of braitschite, $Ca_{6.15}Na_{0.85}RE_{2.08}[B_6O_7(OH)_3(O,OH)_3]_4(H_2O)$, is reported here in space group $P6/m$ with unit-cell parameters $a = 12.1506(6)$, $c = 7.3678(4)$ Å, and $V = 942.03(8)$ Å^3. Data were collected from a single crystal using a Mo$K\alpha$ source and a CCD detector, solved by direct methods, and refined to an R factor of 2.81%. The mineral structure consists of hexaborate fundamental building blocks that polymerize along [001] and are bound by Ca^{2+} and REE^{3+} counterions. The framework forms hexagonal channels, which are occupied alternately by Ca^{2+} cations and water molecules. In an investigation of its thermal stability, braitschite maintains its crystallinity to a temperature of 400 °C, after which it undergoes decomposition. Using Rietveld refinements against powder X-ray diffraction data, we were able to track the loss of water molecules in channels and hydroxyl groups in the covalent B-O network with increasing temperature.

Keywords: Braitschite, borate, rare earth mineral, crystal structure

INTRODUCTION

The crystal chemistry of borate minerals is defined by covalent boron-oxygen bonds, which result in either trigonal or tetrahedral building units that may polymerize to form extended covalent networks (Hawthorne et al. 2002). In addition to building unit variation that results from cluster formation and polymerization in 1, 2, or 3 dimensions, these minerals vary by their level of hydration and the identity of charge-balancing metal cations. Among these cations, rare earth elements (REE) are known to occur in borates and are frequently accompanied by other metal ions of similar size, including Ca^{2+} (Jones et al. 1996).

The physical properties and chemical composition of braitschite, a calcium rare earth borate, were first described in 1968 (Raup et al. 1968). Limited crystallographic data were obtained at the time that allowed determination of the crystal system but no structure solution. Herein, we present the crystal structure of braitschite as solved and refined from single-crystal X-ray diffraction data. This structure solution has a unit cell with dimensions that closely resemble the cell proposed in the original research [proposed: $a = 12.265(1)$, $c = 7.377(5)$, $V = 944.02(13)$ Å^3; this study: $a = 12.1506(6)$, $c = 7.3678(4)$, $V = 942.03(8)$ Å^3]. Moreover, the formula from our structure determination corresponds closely with the chemical analysis performed on samples from the type locality and corrects a problem in the originally proposed formula that precluded crystallization in a hexagonal cell {proposed: $(Ca,Na)_7RE_2(B_{22}O_{43})(H_2O)_7$; this research: $Ca_{6.15}Na_{0.85}RE_{2.08}[B_6O_7(OH)_3(O,OH)_3]_4(H_2O)$}. We additionally report the thermal stability of braitschite, including its hydration level as a function of temperature.

EXPERIMENTAL METHODS

A single crystal of braitschite was obtained from the Gem and Mineral Collection of the Smithsonian Institution's National Museum of Natural History. The braitschite was from the samples collected at the Cane Creek mine near Moab, Utah, described by Raup et al. (1968). The braitschite occurs as fine-grained nodules in anhydrite. Individual crystals are hexagonal plates that in scanning electron microscope images range from ~0.1 to 75 micrometers in diameter. The crystal used for this study was isolated by sieving some of the powdery sample and then searching through the larger size fraction.

The crystal was mounted on a glass fiber, and single-crystal X-ray diffraction data were collected on a Bruker APEXII instrument with a Mo$K\alpha$ source. The instrument was equipped with a CCD detector, and the collection took place at room temperature using 0.5° φ and ω scans. The data were integrated using the APEXII software suite (Bruker 2008a). An empirical absorption correction was applied using SADABS (Sheldrick 2008b), and a ψ correction was applied in XPREP taking into account the crystal habit (Bruker 2008b).

No systematic absences were observed in the data, and structure solution and refinement were pursued using SHELX-97 (Sheldrick 2008a) in space groups suggested by statistics. Among these, $P\bar{3}$ in particular was pursued, as it had the best figure of merit. Subsequent to refinement in this space group, Platon was used to assess for additional symmetry (Spek 2003). An alternative symmetry setting was identified, and the space group was consequently changed to $P6/m$, which yielded an excellent refinement. No additional symmetry was found in this model. Crystallographic and structure-refinement data are summarized in Table 1.

Powder X-ray diffraction was used to complement the single-crystal diffraction data and was performed in conjunction with heating experiments to study the hydration level and thermal stability of braitschite. Powder samples of braitschite (<325 mesh) were loaded into 0.7 mm quartz glass capillaries, and powder X-ray diffraction patterns were collected with a Rigaku D/max Rapid microdiffractometer with an imaging plate detector using Mo$K\alpha$ radiation and 5 min exposures. The sample was rotated during data collection, and the full diffraction rings were integrated by the vendor-supplied program "AreaMax" to produce the final diffraction data used for the Rietveld refinements. Diffraction data were collected at room temperature and for braitschite samples that had been heated successively in air to 110, 300, 400, 500, 600, and 700 °C and then cooled to near room temperature.

Rietveld refinements of the braitschite structures were performed using the EXPGUI interface (Toby 2001) of the General Structure Analysis System (GSAS) (Larson and von Dreele 1994). The initial braitschite structure parameters were those determined by the single-crystal study described above. The background intensities for the X-ray diffraction patterns were fit using up to 15 terms of a shifted Chebyschev function. The peak profiles were modeled by a pseudo-Voigt profile function (Thompson et al. 1987) with asymmetry corrections (Finger et al. 1994) and microstrain anisotropic broadening terms (Stephens 1999). During initial cycles of refinement only the background, scale, peak profile, and unit-cell parameters were allowed to vary. Then the occupancy factors for certain oxygen atoms were refined, followed by all of the atom positions.

TABLE 1. Summary of crystallographic and structure refinement data

Empirical formula	$H_{14}B_{24}O_{52}Ca_{6.15}Na_{0.85}RE_{2.08}$
Formula weight	1677.47
Habit	Hexagonal plate
Color	Pink
T (K)	273
λ (Mo$K\alpha$)	0.71073 Å
Crystal system	Hexagonal
Space group	$P6/m$
a (Å)	12.1506(6)
c (Å)	7.3678(4)
V (Å³)	942.03(8)
Z	1
D_{calc} (g/cm³)	3.168
μ (mm⁻¹)	5.354
R_{int}	0.0675
R_1, wR_2*	0.0371, 0.0768
R_1, wR_2* [$I > 2\sigma(I)$]	0.0281, 0.0742
GOOF	1.068

* $R_1 = \Sigma||F_o| - |F_c||/\Sigma|F_o|$; w$R_2 = \{\Sigma[w(F_o^2 - F_c^2)^2/\Sigma[w(F_o^2)^2]\}^{1/2}$.

a

b

FIGURE 1. (**a**) Braitschite's topology is based on a hexaborate FBB, shown here as a polyhedral representation, which contains two crystallographically unique B sites and six O sites. (inset) The FBB forms a chain in the extended structure, with polymerization occurring alternately through the circled and uncircled tetrahedra. (**b**) A polyhedral view of the chain shows how hexaborate FBBs polymerize down [001] to form a chain.

Thermal stability was also investigated using thermogravimetric analysis (TGA). TGA was performed on a Perkin Elmer Pyris1 under nitrogen with a 10 °C/min temperature ramp from 30 to 800 °C.

RESULTS

The covalent framework of braitschite is generated by atoms B1 and B2, the symmetry equivalents of which account for all the B atoms in the mineral. B1 is coordinated to four O atoms (O1, O4¹⁰, O5, O6; 10 = –x + y, –x + 1, z), of which O6 is a hydroxyl group, according to bond valence summation values for O atoms summarized in Table 2 (Brese and O'Keeffe 1991; Trzesowska et al. 2006). B2 is likewise bound to four O atoms (O1, O2, O3, O4), of which O3 is μ3 (coordinated to three boron atoms). Figure 1, with B and O sites labeled, shows the connectivity of the hexaborate fundamental building block (FBB), which polymerizes to form chains that propagate down [001].

Charge-balancing cations separate the anionic borate clusters. These include one Ca^{2+} cation (Ca1) and one REE^{3+} cation between adjacent FBBs. Ca1 sites experience some substitutional disorder with Na^+ cations (Na1). Channels down [001] that are created by this charge-balancing network are occupied alternately by Ca^{2+} ions in the second unique Ca site (Ca2) and water molecules (OW1). Refer to Table 3 for a list of atomic coordinates and displacement parameters. Important bond distances and angles are summarized in Table 4, and the mineral's structure is shown in Figure 2. A CIF[1] is available on deposit.

The ratio of REE was fixed according to the elemental composition determined by Raup et al. (1968) and is summarized in Table 5. The total site occupancy was then allowed to refine freely, giving 69% occupancy or 2.08 RE^{3+}/unit cell. Full occupancy of this crystallographic site would suggest a formula with 3 REE atoms per unit cell. Partial occupancy of the site, however, accounts for the 2 REE atoms per unit cell that were previously reported (Raup et al. 1968). As with the REE site, substitutional disorder of the Ca1 site was modeled in the crystal structure based on the previously reported compositional data,
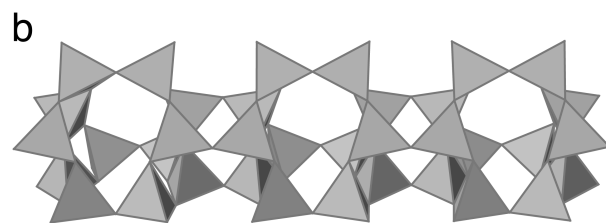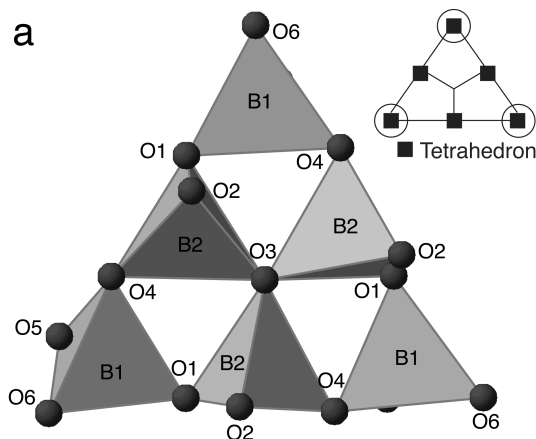
TABLE 2. Bond valence sums for O in braitschite

O1	1.58
O2	2.08
O3	2.09
O4	1.83
O5	1.91
O6	1.13

TABLE 3. Atomic coordinates (×10⁴) and equivalent isotropic displacement parameters (Å² × 10³) for braitschite

	x	y	z	U_{eq}
RE	5000	5000	5000	13(1)
Ca1	3147(1)	3124(1)	0	11(1)
Na1	3147(1)	3124(1)	0	11(1)
Ca2	10000	10000	–5000	54(1)
O1	3256(2)	4818(2)	3134(3)	16(1)
O2	3690(3)	5215(3)	0	15(1)
O3	3333	6667	1848(5)	13(1)
O4	5239(2)	6539(2)	2199(3)	17(1)
O5	1340(3)	3831(3)	5000	20(1)
O6	1418(2)	2877(2)	2110(3)	24(1)
B1	1877(3)	4115(3)	3205(5)	15(1)
B2	3894(3)	5808(3)	1757(5)	15(1)
OW1	10000	10000	0	57(3)

wherein the mineral was found to contain CaO (21.8%) and Na_2O (1.68%). Ca/Na substitutional disorder was originally modeled in the channel (at the Ca2 site), but the refinement improved when this disorder was instead modeled at the framework site (Ca1).

Powder diffraction patterns, shown in Figure 3, for samples heated up to and including 400 °C are similar to each other, but

[1] Deposit item AM-11-003, CIF. Deposit items are available two ways: For a paper copy contact the Business Office of the Mineralogical Society of America (see inside front cover of recent issue) for price information. For an electronic copy visit the MSA web site at http://www.minsocam.org, go to the *American Mineralogist* Contents, find the table of contents for the specific volume/issue wanted, and then click on the deposit link there.

TABLE 4. Selected bond distances (Å) and angles (°)

	Distance (Å)		Angle (°)
B1-O1	1.452(4)	O5-B1-O1	115.1(3)
B1-O6	1.545(4)	O5-B1-O4[10]	108.0(3)
B1-O5	1.438(4)	O1-B1-O4[10]	112.5(3)
B1-O4[10]	1.485(4)	O5-B1-O6	110.3(3)
B2-O1	1.467(4)	O1-B1-O6	107.7(2)
B2-O2	1.441(4)	O4[10]-B1-O6	102.6(2)
B2-O3	1.505(4)	O2-B2-O4	111.5(3)
B2-O4	1.455(4)	O2-B2-O1	108.9(3)
Ce1-O1	2.440(2)	O4-B2-O1	108.5(2)
Ce1-O4	2.701(2)	O2-B2-O3	111.3(3)
Ce1-O5[4]	2.643(3)	O4-B2-O3	109.0(2)
Ca1-O1	3.054(2)	O1-B2-O3	107.5(3)
Ca1-O2	2.284(3)	B1-O5-B1[1]	133.7(3)
Ca1-O4[3]	2.416(2)	B1-O1-B2	119.1(2)
Ca1-O6[7]	2.440(2)	B2-O4-B1[5]	126.4(2)
		B2[10]-O3-B2	119.80(3)
		B2-O2-B2[9]	127.8(3)

Note: Symmetry transformations: 1 = x, y, −z + 1; 3 = x, y, −z + 1; 4 = y, −x + y, −z + 1; 5 = −y + 1, x − y + 1, z; 7 = y, −x + y, −z; 9 = x, y, −z; 10 = −x + y, −x + 1, z.

TABLE 5. Distribution of cations in braitschite

M_xO_n	M^{n+}/unit cell	wt% observed	wt% calculated
$\Sigma CaO + Na_2O$	7	23.48	22.17
CaO	6.15	21.8	20.6
Na_2O	0.85	1.68	1.57
ΣRE_2O_3	2.08	20.57	20.22
Y_2O_3	0.15	1.50	1.01
La_2O_3	0.46	4.57	4.47
Ce_2O_3	0.77	7.64	7.54
Pr_2O_3	0.10	1.00	0.985
Nd_2O_3	0.37	3.67	3.72
Sm_2O_3	0.10	0.941	1.04
Eu_2O_3	0.04	0.390	0.420
Gd_2O_3	0.03	0.320	0.325
Tb_2O_3	0.01	0.103	0.109
Dy_2O_3	0.03	0.250	0.334
Ho_2O_3	0.01	0.054	0.113
Er_2O_3	0.01	0.081	0.114
Tm_2O_3	<0.01	0.023	0.016
Yb_2O_3	<0.01	0.018	0.013
Lu_2O_3	<0.01	0.010	0.007

Notes: wt% observed is based on bulk analysis (Raup et al. 1968) and wt% calculated is from the assignments in this crystallographic model.
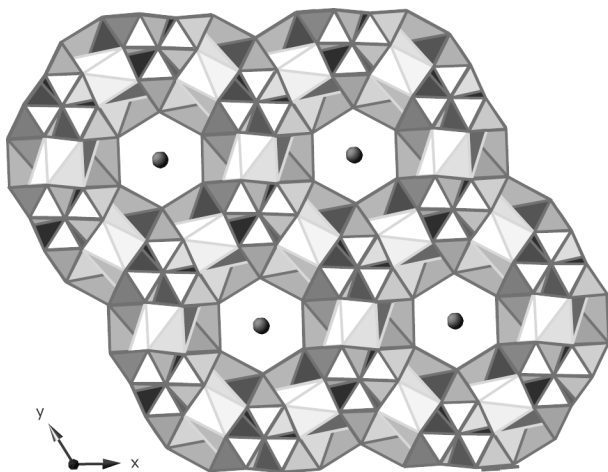

FIGURE 2. A polyhedral representation of braitschite down [001] shows the FBB (darkest polyhedra) separated by charge-balancing Ca^{2+} (bordering the channels) and RE^{3+} ions (lightest polyhedra). Channels down [001] are occupied by alternating Ca^{2+} ions and H_2O molecules.
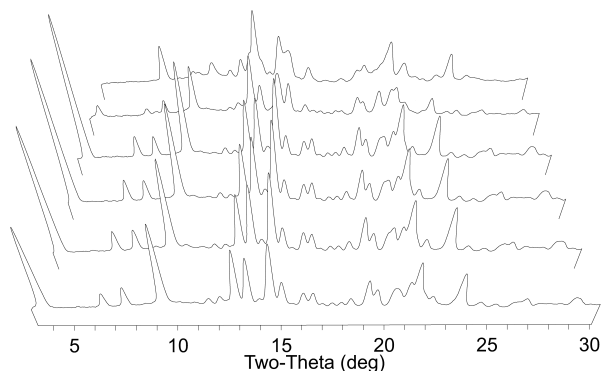

FIGURE 3. Powder X-ray diffraction patterns of braitschite collected after heating and returning the sample to near room temperature are shown here to 30 °2θ. Patterns from front to back are for samples heated to 110, 300, 400, 500, 600, and 700 °C, respectively.

those collected for samples heated to higher temperatures suggest that the structure undergoes major changes above approximately 500 °C. After heating to 700 °C, braitschite is no longer evident in the powder pattern, suggesting complete breakdown or transformation of the structure. We attribute the 700 °C diffraction pattern to several phases, including a calcium borate (PDF 78-1277) and rare earth oxide, RE_2O_3 (e.g., Eu_2O_3, PDF 76-0154) (ICDD 1998). Not all phases in the decomposition products have been identified.

The occupancy factors for the tunnel water, OW1, and the hydroxyl group, O6, were refined on data sets collected for unheated braitschite and for samples heated to 110, 300, and 400 °C. Tunnel water is lost by about 400 °C, and probably correlates with the weight loss observed by TGA (Fig. 4). It also appears that starting at 300 °C and continuing to 400 °C, there is a loss of hydroxyl water from O6. The O6 occupancy continues to decrease at 500 °C, but significant changes in the diffraction pattern after heating to this temperature make the Rietveld refinement results less certain. These results are summarized in Table 6.

DISCUSSION

The formula that was proposed for braitschite based on previous chemical analysis (Raup et al. 1968) is unable to account for mineral's hexagonal space group, as the B and O atoms cannot divide evenly into a hexagonal cell.

$$(Ca,Na_2)_7RE_2(B_{22}O_{43})(H_2O)_7. \tag{1}$$
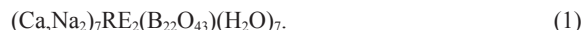
A second formula that assumes a greater degree of contamination in the mineral sample was also proposed.

$$(Ca,Na_2)_6RE_2[B_{24}O_{45}](H_2O)_6. \tag{2}$$
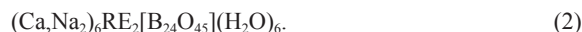
Based on this crystallographic analysis, we suggest the following formula:

$$Ca_{6.15}Na_{0.85}RE_{2.08}[B_6O_7(OH)_3(O,OH)_3]_4(H_2O). \tag{3}$$
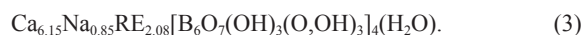
Formula 3 agrees more closely with formula 1 with respect to the metal cations, but also clearly indicates that the B and O values are more accurately represented in formula 2. Fur-

thermore, the amount of free water in this crystal structure is much less than was proposed in either formulas 1 or 2, with the discrepancy made up in hydroxyl groups and oxygen atoms in the covalent 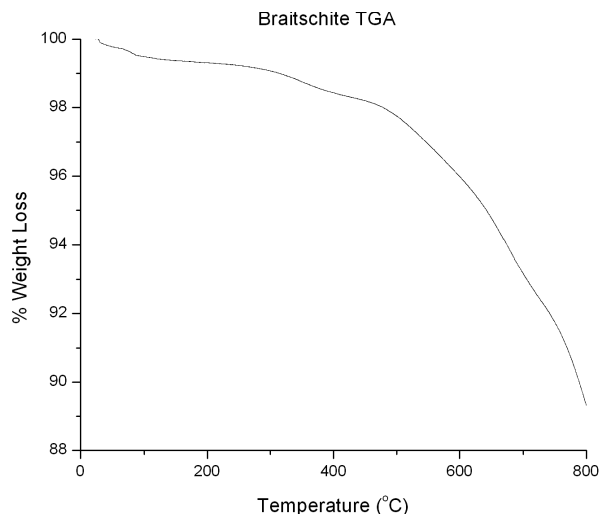B-O network in formula 3. Any charge resulting from disorder of Ca^{2+} and Na^+ ions and the partial occupancy of the REE site is corrected through changes in protonation in the covalent B-O framework. In particular, O1 exhibits partial hydroxyl character (Table 2).

Assignment of the Ca/Na ratio in formula 3 was based on elemental analysis from the previous study, but refinement of this value suggests that the crystal from which our data were collected may be much higher in Ca than the bulk. This was determined by assuming that the Ca1 site was fully occupied by a combination of Ca^{2+} and Na^+ cations. The ratio of the two was then permitted to refine, while the total site occupancy was fixed at one. This resulted in a 96% Ca contribution to the site, which, when considered with the Ca2 site, gives rise to a total of approximately 97% Ca in the sample. In contrast, the elemental analysis reported 88% Ca distributed over the two sites. It is important to note that the values in the final refinement were ultimately fixed to the levels reported in the elemental analysis.

Although symmetry transformations give 3 RE^{3+} sites per unit cell, free refinement of the occupancy gives us a 69% occupied site. This translates to 2.08 RE^{3+} cations per unit cell. The occupancy assumes the relative amounts of REE are the same as determined by the chemical analysis for the bulk sample. Thus, if the composition of the crystal differs from that of the bulk, the site occupancy factor could vary from as little as 53% (when all REE is modeled as Lu) to over 100% (Y). Based on the consistency between the bulk analysis and the data from this single crystal, we expect approximately 2 REE per unit cell to be representative.

A more general formula for braitschite that reflects variations in the Ca/Na ratio and that fixes the REE occupancy is shown below in formula 4:

$$(Ca,Na)_7RE_2[B_6O_7(OH)_3(O,OH)_3]_4(H_2O). \qquad (4)$$

As in formula 3, variations in charge that result from disorder of Ca^{2+} and Na^+ ions in formula 4 are canceled by protonation or deprotonation of O1.
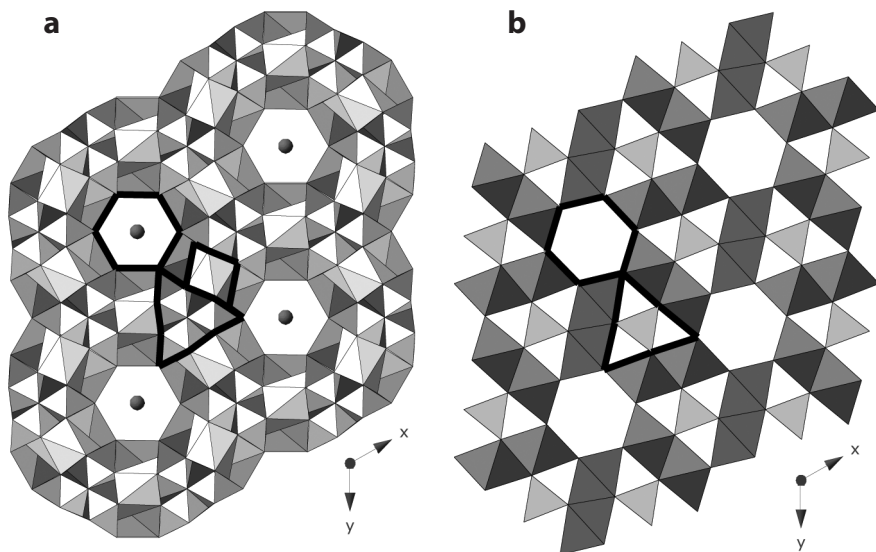

FIGURE 4. Plot of TGA shows only slight weight loss up to 400 °C that corresponds with the loss of water from OW1 and O6 sites. At higher temperatures, the sample undergoes further decomposition and associated weight loss.

TABLE 6. Unit-cell parameters and occupancy factors for OW1 and O6 with heating

	Unit cell		Occupancy factor	
T (°C)	a	c	OW1	O6
23	12.151(1)	7.375(1)	1.00	1.00
110	12.154(1)	7.376(1)	1.00	1.00
300	12.138(1)	7.386(1)	0.36(1)	0.96(1)
400	12.129(1)	7.389(1)	0.07(2)	0.91(1)
500*	12.112(1)	7.400(1)	0.49(3)	0.79(1)

* Change in the powder pattern that could be indicative of structural changes makes the accuracy of this data uncertain.

◄**FIGURE 5.** The topology of braitschite (**a**) resembles that of fluoborite (**b**). Both structures contain hexagonal channels and have FBBs that occupy a triangular area within the framework (shown in bold). Braitschite additionally contains a REE "spacer," also outlined, between the cations that frame the channels.

The mineral with a structure most similar to braitschite is fluoborite, $Mg_3(BO_3)(F,OH)_3$ (Dal Negro and Tadini 1974; Takéuchi 1950). Both contain hexagonal channels bordered by metal cations. Whereas in fluoborite these channels are vacant, in braitschite they are occupied by Ca^{2+} cations and water. The covalent structures of the two minerals further differ in their FBB. While both occupy a triangular space that joins three channels, a monomeric species exists in fluoborite in contrast to the polymerized hexaborate FBB in braitschite. The REE site between Ca^{2+} cations in braitschite acts as a spacer to make room for this larger FBB. Similarities between the two are highlighted in Figure 5.

The primary difference between braitschite and fluoborite lies in the structure of the FBB, the repeated polyhedral borate clusters that have traditionally been used to define the structures of these minerals (Burns et al. 1995; Hawthorne 1983; Hawthorne et al. 2002; Yuan and Xue 2007). According to the classification guidelines laid out by Yuan and Xue (2007), the FBB of braitschite may be described as a hydrous big-bridge-ring chain, wherein we observe polymerization along [001]. To our knowledge this FBB has not previously been observed in a naturally occurring borate, although it has been seen in synthetic rare earth borates (Emme et al. 2004). The FBB, shown in detail in Figure 1, is composed of six tetrahedral units with a μ3 oxygen located at its center. Polymerization occurs alternately through the tetrahedra located at the FBB's corners and the tetrahedra along the FBB's edges and adds a dimension of complexity to braitschite that fluoborite lacks.

ACKNOWLEDGMENTS

REFERENCES CITED

Brese, N.E. and O'Keeffe, M. (1991) Bond valence parameters for solids. Acta Crystallographica, Section B, 47, 192–197.
Bruker (2008a) APEXII Software Suite. Bruker AXS, Madison, Wisconsin.
——— (2008b) XPREP. Bruker AXS, Madison, Wisconsin.
Burns, P.C., Grice, J.D., and Hawthorne, F.C. (1995) Borate minerals. I. Polyhe-dral clusters and fundamental building blocks. Canadian Mineralogist, 33, 1131–1151.
Dal Negro, A. and Tadini, C. (1974) Refinement of the crystal structure of fluo-borite, $Mg_3(F,OH)_3(BO_3)$. Tschermaks Mineralogische und Petrographische Mitteilungen, 21, 94–100.
Emme, H., Nikelski, T., Schleid, T., Poettgen, R., Moeller, M.H., and Huppertz, H. (2004) High-pressure synthesis, crystal structure, and properties of the new orthorhombic rare-earth meta-oxoborates $RE(BO_2)_3$ (RE=Dy-Lu). Zeitschrift für anorganische und allgemeine Chemie, 59, 202–215.
Finger, L.W., Cox, D.E., and Jephcoat, A.P. (1994) A correction for powder dif-fraction peak asymmetry due to axial divergence. Journal of Applied Crystal-lography, 27, 892–900.
Hawthorne, F.C. (1983) Graphical enumeration of polyhedral clusters. Acta Crystal-lographica, Section A, 39, 724–736.
Hawthorne, F.C., Burns, P.C., and Grice, J.D. (2002) The crystal chemistry of boron. In E.S. Grew and L.M. Anovitz, Eds., Boron: Mineralogy, Petrology, and Geochemistry, 33, 41–115. Reviews in Mineralogy, Mineralogical Society of Washington, Chantilly, Virginia.
ICDD (1998) PDF-2. W.F. McClune, Ed., Joint Committee for Powder Diffrac-tion Standards-International Centre for Diffraction Data, Newton Square, Pennsylvania.
Jones, A.P., Wall, F., and Williams, C.T. (1996) Rare earth minerals: Chemistry, origin and ore deposits, p. 1–17. Chapman and Hall, London.
Larson, A.C. and von Dreele, R.B. (1994) GSAS-General Structure Analysis System. Los Alamos National Laboratory (LAUR 86-748).
Raup, O.B., Gude, A.J., Dwornik, E.J., Cuttitta, F., and Rose, H.J. (1968) Braitsch-ite, a new hydrous calcium rare-earth borate mineral from the Paradox Basin, Grand County, Utah. American Mineralogist, 53, 1081–1095.
Sheldrick, G. (2008a) A short history of SHELX. Acta Crystallographica, Section A, 64, 112–122.
——— (2008b) SADABS. University of Gottingen, Gottingen, Germany.
Spek, A.L. (2003) Single-crystal structure validation with the program PLATON. Journal of Applied Crystallography, 36, 7–13.
Stephens, P.W. (1999) Phenomenological model of anisotropic peak broadening in powder diffraction. Journal of Applied Crystallography, 32, 281–289.
Takéuchi, Y. (1950) The structure of fluoborite. Acta Crystallographica, 3, 208–10.
Thompson, P., Cox, D.E., and Hastings, J.B. (1987) Rietveld refinement of Debye-Scherrer synchrotron X-ray data from Al_2O_3. Journal of Applied Crystallography, 20, 79–83.
Toby, B.H. (2001) EXPGUI, a graphical user interface for GSAS. Journal of Ap-plied Crystallography, 34, 210–213.
Trzesowska, A., Kruszynski, R., and Bartczak, T.J. (2006) Bond-valence parameters of lanthanides. Acta Crystallographica, Section B, 62, 745–753.
Yuan, G. and Xue, D. (2007) Crystal chemistry of borates: The classification and algebraic description by topological type of fundamental building blocks. Acta Crystallographica, Section B, 63, 353–362.